Spatiotemporal Associations between GOES Aerosol Optical Depth Retrievals and Ground-Level $PM_{2.5}$

CHRISTOPHER J. PACIOREK,*,† YANG LIU,‡ HORTENSIA MORENO-MACIAS,‡ AND SHOBHA KONDRAGUNTA§

Department of Biostatistics and Department of Environmental Health, Harvard School of Public Health, Boston, Massachusetts 02115, and National Oceanic and Atmospheric Administration, Camp Springs, Maryland 20746

Received December 19, 2007. Revised manuscript received April 12, 2008. Accepted May 7, 2008.

We analyze the strength of association between aerosol optical depth (AOD) retrievals from the GOES aerosol/smoke product (GASP) and ground-level fine particulate matter ($PM_{2.5}$) to assess AOD as a proxy for $PM_{2.5}$ in the United States. GASP AOD is retrieved from a geostationary platform, giving half-hourly observations every day, in contrast to once per day snapshots from polar-orbiting satellites. However, GASP AOD is based on a less-sophisticated instrument and retrieval algorithm. We find that daily correlations between GASP AOD and $PM_{2.5}$ over time at fixed locations are reasonably high, except in the winter and in the western U.S. Correlations over space at fixed times are lower. Simple averaging to the month and year actually reduces correlations over space, but statistical calibration allows averaging over time that produces moderately strong correlations. These results and the data density of GASP AOD highlight its potential to help improve exposure estimates for epidemiological analyses. On average 39% of days in a month have a GASP AOD retrieval compared to 11% for MODIS and 5% for MISR. Furthermore, GASP AOD has been retrieved since November 1994, providing a long-term record that predates the availability of most $PM_{2.5}$ monitoring data and other satellite instruments.

1. Introduction

Epidemiological studies provide evidence that chronic exposure to particulate matter (PM) is related to increased mortality, as well as outcomes such as ischemic heart disease, dysrhythmias, heart failure, cardiac arrest, and lung cancer (*1–4*). Studies of the chronic health effects of PM rely on spatial heterogeneity in PM concentrations to estimate the effects. A combination of spatial modeling and land use regression can improve estimation of concentrations at fine scales by using covariate information to help estimate concentrations at locations far from monitors (*5*), but efforts often suffer from the sparse spatial representation in the monitoring network. Evidence of health effects of acute exposure to PM (*6, 7*) relies on temporal heterogeneity in PM, but the every third (or sixth) day schedule at many monitors reduces statistical power in these time series studies.

Remote sensing holds promise for adding information for exposure estimation, particularly spatial information in suburban and rural areas far from monitors, and temporal information on days without monitoring. Satellite-derived aerosol optical depth (AOD) is correlated with ground-level PM (*8–12*), specifically particles with diameter ranging from 0.05−2 μm (*13*), which is roughly the definition of $PM_{2.5}$ (particles with aerodynamic diameter less than 2.5 μm), the size fraction on which current EPA regulatory efforts focus. These correlations occur despite the mismatch in vertical detail between total column aerosol, as measured by AOD, and ground-level $PM_{2.5}$, the level of interest for health studies. One approach to help account for the mismatch is calibration via a regression model based on season, spatial location, and meteorological information (*10*).

Efforts to use AOD as a proxy for $PM_{2.5}$ have concentrated on the multiangle imaging spectroradiometer (MISR) and moderate resolution imaging spectroradiometer (MODIS) instruments. These are on polar-orbiting satellites, which causes relatively sparse coverage over time, with individual locations in the eastern United States sampled via a single snapshot every 4−7 (1−2) days by MISR (MODIS). Combined with a high proportion of missing retrievals because of cloud cover, this causes sparse coverage in space and time that can impede use in health studies. Geostationary satellites provide much more complete data; the GOES aerosol/smoke product (GASP) AOD provides observations every 30 min on a nominal 4 km grid, finer nominal resolution than the MODIS or MISR grids. However, the GASP AOD retrievals are less precise than those from the polar-orbiting instruments because of the coarse spectral resolution and fixed viewing geometry of the sensor (*14*). Since GASP AOD retrievals use only the visible channel, all atmospheric and aerosol properties (e.g., size distribution, composition, and scattering phase function) must be assumed, and only AOD is allowed to vary in the radiative transfer model. Despite these limitations, GASP AOD retrievals are reasonably well-correlated with AERONET ground measurements of total column aerosol (*14, 15*), albeit less precise than MODIS, or particularly MISR (*15*). To date, no studies have been done to understand the relationship between GASP AOD and ground-level $PM_{2.5}$.

Here we assess the potential of GASP AOD to act as a proxy for daily, monthly, and yearly ground-level $PM_{2.5}$, focusing on these time scales because of their relevance for epidemiological studies. First, we assess the basic strength of association between GASP AOD and $PM_{2.5}$ in space and time. We build flexible regression-style models to calibrate daily AOD to $PM_{2.5}$ based on meteorological, spatial, and temporal effects. We compare the association of calibrated AOD with daily, monthly, and yearly average $PM_{2.5}$. Our goal is to understand the association of GASP AOD with $PM_{2.5}$ and show how to calibrate GASP AOD to increase its utility, not to physically interpret our statistical modeling of AOD. Finally, we assess whether the absence of an AOD retrieval is associated with the $PM_{2.5}$ concentration, to determine if bias is induced by ignoring the missingness and simply using the available retrievals.

2. Data and Methods

2.1. Data. We make use of GASP AOD from GOES-12 (East) imager data for the year 2004, provided by the U.S. National Oceanic and Atmospheric Administration (NOAA). Prados

* Corresponding author fax: 617-432-5619; e-mail: paciorek@alumni.cmu.edu.

† Department of Biostatistics, Harvard School of Public Health.

‡ Department of Environmental Health, Harvard School of Public Health.

§ National Oceanic and Atmospheric Administration.

10.1021/es703181j CCC: $40.75
Published on Web 06/28/2008

et al. (*14*) describe the GOES-12 imager data and GASP AOD algorithm in detail. In brief, AOD is calculated from a single visible channel (520−720 nm) based on assumptions about surface reflectivity and atmospheric and aerosol properties, while the cloud mask is determined from infrared channels 2 (3.9 um) and 4 (10.7 um) and the visible channel. The pixel centroids of the AOD retrievals are nominally on a 4 km grid, but the distance between centroids is not generally 4 km. Retrievals are attempted every half-hour, but cloud cover and high surface reflectivity lead to many missing observations.

GASP AOD (henceforth referred to as AOD) retrievals are available during daylight, from 10:45−23:45 UTC. In our core analysis, we follow NOAA's criteria for screening valid AOD observations, described in the Supporting Information. The Supporting Information provides sensitivity analyses suggesting we can relax some of these criteria. Negative retrievals occur due to errors in the estimation of surface reflectivity when AOD is low. Unlike Prados et al. (*14*), we make use of negative retrievals in the hope that they indicate low AOD. The Supporting Information shows that including these retrievals provides useful information.

To assess the relationship between $PM_{2.5}$ and AOD, we matched monitoring data from the US EPA Air Quality System (AQS) to the nearest GOES pixel, omitting a small number of monitors for which the nearest pixel centroid is closer to another monitor. Since we use AOD as the dependent variable in our regression modeling, this avoids having duplicate AOD values. We then selected days for which the EPA monitor reported a $PM_{2.5}$ concentration. Our interest is in fine resolution estimation of $PM_{2.5}$, so unlike other analyses we use individual pixels instead of aggregating AOD across adjoining pixels. We calculate a daily estimate of AOD as the simple average of the available retrievals but consider another approach in the Supporting Information. We have 99 159 matched daily observations, of which 46 684 have at least one valid AOD retrieval during the day. Of the matched observations with valid AOD retrievals, 6558 are in winter, with 13 361, 15 454, and 11 311 in spring (March-May), summer (June-August), and fall (September−November), respectively.

We use data with EPA parameter 88101. This excludes most $PM_{2.5}$ data from IMPROVE sites, which are generally in very rural areas, avoiding issues of comparability between AQS and IMPROVE observations and focusing our calibration efforts on populated areas where people live. We included all observations regardless of any quality flags in the data record, at the suggestion of EPA personnel (Michael Papp, personal communication) who indicate that all data reported to AQS should be valid data. For simplicity, we used only data with parameter occurrence code equal to one, thereby including only the primary monitor at a site. AQS data are the primary data used for estimating exposure in epidemiological studies, so we consider them as the gold standard here, while acknowledging that the ground measurements are not error-free (instrument error variance of approximately 1.5 based on colocated monitors, relative to a trimmed variance of the measurements of 60). We also make use of local land use and monitoring objective information that EPA provides for many of the monitors.

For meteorological information, we concentrate on planetary boundary layer (PBL, i.e., mixing height) and relative humidity (RH) as key variables that affect the relationship between $PM_{2.5}$ and AOD (*10*). PBL is used to represent the vertical distribution of $PM_{2.5}$; most particle mass loading resides in the lower troposphere, and the PBL gives an indication of how much of the column is more actively mixed and relatively homogeneous. Higher PBL is expected to be associated with a larger ratio of AOD to $PM_{2.5}$ because aerosol emitted from the surface is distributed over a larger volume of air. The size of hygroscopic particles such as sulfates and organic carbonaceous species grows with increasing relative humidity, resulting in greatly increased light extinction efficiency. Since $PM_{2.5}$ is measured as dry particle mass (measured at controlled RH of approximately 40%) we expect higher RH to be associated with a larger ratio of AOD to $PM_{2.5}$. We use the North American Regional Reanalysis (NARR) meteorological fields; the NARR assimilates available data with a state-of-the-art meteorological model to estimate meteorological parameters every 3 h on a 32 km grid covering North America. Rogers et al. (*16*) report that NARR PBL is highly correlated with LIDAR measurements, although in urban areas the correlation decreases. We use data from 12:00, 15:00, 18:00, and 21:00 UTC to match the time range of the AOD retrievals, and we take the inverse-squared distance weighted averages of the values from the four closest grid points to each EPA monitor as simple estimates of the already-smooth model output fields at the monitor sites.

In principle, since AOD is at the half-hourly resolution, one might calibrate to hourly $PM_{2.5}$ measurements from AQS. However, the number of hourly monitors is much smaller than daily monitors, limiting our ability to calibrate AOD to hourly $PM_{2.5}$, and there is no federal reference method (FRM) for hourly $PM_{2.5}$. The relationship of hourly $PM_{2.5}$ (averaged to the day) to daily FRM measurements can vary by location and season of year, as is evident in the AQS data, suggesting the need to calibrate hourly $PM_{2.5}$ to daily $PM_{2.5}$. This occurs in part because of the loss of semivolatile compounds in continuous $PM_{2.5}$ measurements. For simplicity and because our interest is in relationships between $PM_{2.5}$ and AOD at time scales longer than hourly (note that the EPA air quality standard is a 24-h average), we restrict our analysis to daily associations based on daily FRM monitors and daily average AOD.

Associations of AOD and $PM_{2.5}$ are weak in the western U.S. (Section 3.2), so most of our results are reported for the area east of 100 °W.

2.2. Statistical Calibration Model. We build a statistical regression model to understand the factors that modify the relationship between AOD and $PM_{2.5}$. Using the model we calculate a calibrated AOD variable that is more strongly associated with $PM_{2.5}$. Ultimately, as part of our larger research effort, the calibrated AOD will be used in a statistical prediction model for $PM_{2.5}$.

Liu et al. (*10*) treat $PM_{2.5}$ as the dependent (response) variable in regression models, using the log transform of both AOD and $PM_{2.5}$ to create an additive model on the log scale. Here we consider log AOD as the dependent variable and regress on $PM_{2.5}$ and other factors, treating AOD as observed data. We take this approach in part because of the high variability in AOD, reflecting its noisiness as a proxy for $PM_{2.5}$, and the varying number of retrievals contributing to average daily AOD. These are difficult to account for if AOD is considered to be the independent variable. Using the less error-prone variable as the dependent variable also helps avoid bias (toward zero) in the estimated regression coefficient. Furthermore, our goal is to understand AOD as a proxy for $PM_{2.5}$. Using $PM_{2.5}$ as the dependent variable places the focus on including other variables that help to explain $PM_{2.5}$, the focus of a large body of environmental health research, rather than assessing the association of $PM_{2.5}$ and AOD. In our models the observed $PM_{2.5}$ values at the monitors stand in for true $PM_{2.5}$, ignoring any monitor instrument error.

We considered a variety of models building on Liu et al. (*10*) but using smooth regression functions (*17*) in place of linear functions and indicator variables for region and season. After a model comparison process described in the Supporting Information, we arrived at the final model,

$$\log \bar{a}_{it} \sim N(\mu + g(s_i) + f_t(t) + f_{PBL}(PBL_{it}) + f_{RH}(RH_{it}) + \beta PM_{it}, \tau^2) \quad (1)$$

Here μ is an overall mean (simple additive bias). $g(s_i)$, $f_t(t)$, $f_{PBL}(PBL_{it})$, and $f_{RH}(RH_{it})$ are smoothly varying regression functions that account for additive bias due to spatial location, s_i (represented in the Albers equal-area projection), time (day of year), PBL, and RH, respectively. β is a multiplicative bias coefficient that scales from units of $PM_{2.5}$ to unitless AOD, and PM_{it} is the matched $PM_{2.5}$ measurement. We use the simple average of the available AOD retrievals in each day, $\bar{a}_{it}$, but in the Supporting Information we consider a more sophisticated approach. Since there are negative retrievals, we added 0.6 to each daily mean and then log transformed (the minimum value is −0.5, so adding 0.6 avoids a long left tail after transformation). Using $\bar{a}_{it}$ in place of log $\bar{a}_{it}$ gave similar results but residuals that were slightly more skewed. Fitting separate models of the form in equation 1 for each season, we estimated β to be 0.0018 (95% confidence interval of (0.0010, 0.0027)) in winter, 1 order of magnitude smaller than 0.0164 (0.0157, 0.0170) in spring, 0.0164 (0.0158, 0.0169) in summer, and 0.0129 (0.0123, 0.0134) in fall. Because of the near-zero coefficient for winter we chose to fit models only for spring, summer, and fall. We fit separate models of the form in equation 1 for each season, to facilitate computations with such a large data set and to allow the relationships to vary by season.

The model in equation 1 can be fit in the statistical software, R, using the gam() function, designed for fitting generalized additive models (*17*). The software uses penalized splines to parametrize the smooth functions of time, space, and covariates, allowing for nonlinear relationships. Multiple penalty terms are estimated from the data using extensions of generalized cross-validation (*17*), thereby ensuring that the functions are sufficiently smooth to avoid overfitting and provide generalizability. However, based on model comparisons described in the Supporting Information, we restrict the flexibility of the function of time, giving fitted functions, $\hat{f}_t(t)$, with 3−4 degrees of freedom for each season.

Having fit the model and estimated the smooth functions, we create a calibrated AOD variable, a^*_{it}, by subtracting off the values of all the fitted functions from the observed value, log $\bar{a}_{it}$, except for $PM_{2.5}$:

$$a^*_{it} = \log \bar{a}_{it} - \hat{\mu} - \hat{g}(s_i) - \hat{f}_t(t) - \hat{f}_{PBL}(PBL_{it}) - \hat{f}_{RH}(RH_{it}) \quad (2)$$

Our hope is that by adjusting for factors that modify the relationship of AOD and $PM_{2.5}$, the calibrated AOD (which we note is on a different scale than raw AOD) is more strongly associated with $PM_{2.5}$ than raw AOD and has a reasonably linear relationship. Linearity is preserved when averaging to longer time scales,

$$\frac{1}{T}\sum_{t=1}^{T} a^*_{it} \approx \beta_0 + \beta_1 \frac{1}{T}\sum_{t=1}^{T} PM_{it}, \quad (3)$$

which may produce more robust proxy estimates of $PM_{2.5}$ that average over short-term fluctuations. One would then use time-averaged a^*_{it} as one of a collection of covariates to develop a statistical prediction model with $PM_{2.5}$ as the dependent variable (*5*) where the scaling represented by β_0 and β_1 would be estimated within the prediction model.

To address potential overfitting in our regression model, we divided the data into 10 random sets, each set containing all the observations over time from approximately one-tenth of the locations. We left the tenth set in reserve for final testing and used the other nine sets in a cross-validation approach. We sequentially left out one of the nine sets, fit the model to the remaining eight sets, and calculated calibrated AOD for the observations in the held-out set. Aggregating over the nine sets, this gives us cross-validated values of calibrated AOD for the nine sets that we can correlate with the held-out $PM_{2.5}$ observations.

3. Analyses

3.1. Retrieval Availability. To assess the data density for GASP AOD compared to MODIS and MISR, we calculated the proportion of days in a month with a valid AOD retrieval for each of the three instruments for all AQS sites in the eastern U.S, using the sites as a rough reflection of the population distribution. We matched each of the AQS sites to the nearest pixel for GOES and, on a day-to-day basis, to pixels within a nominal pixel radius of 12.4 km for MISR and 7.1 km for MODIS. MISR (MODIS) provided a valid retrieval on average only 5% (11%) of the days in a given month at a given location. In contrast, GOES provided a valid retrieval on average 39% of the days (21% of days if only considering days with at least five retrievals), assuming no valid retrievals in winter because of the lack of association between GASP AOD and $PM_{2.5}$ (Sections 2.2 and 3.2). Restricting to non-winter, 52% of days have a valid GOES retrieval (28% when requiring at least five retrievals in a day) compared to 12% for MODIS and 5% for MISR.

3.2. Spatiotemporal Associations between Daily AOD and $PM_{2.5}$. Figure 1 plots raw correlations calculated over time for each pixel-monitor match. The correlations are much higher in the eastern than western U.S., as has been found for both MODIS (*9*) and MISR (*10*), and as expected based on higher surface reflectivity in the (less-vegetated) western U.S. Also, with the exception of California, a higher proportion of the aerosol in the west is in the free troposphere, with less local anthropogenic pollution than the east (*18*). Correlations vary by season, with lower correlations (and few retrievals) during winter, while summer, spring, and fall (see Supporting Information) have similar correlations to the all season results.

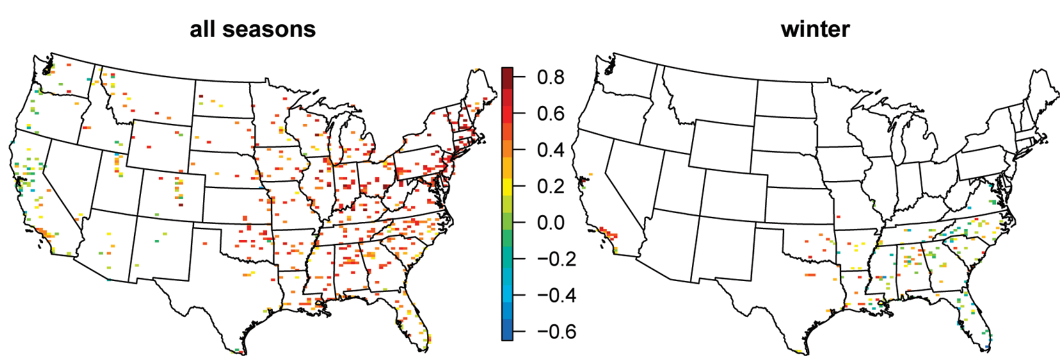

FIGURE 1. Correlations at individual sites between daily average $PM_{2.5}$ and the average of half-hourly AOD retrievals for all seasons (left) and winter only (right). Plots are based on site-days with at least three AOD retrievals, and only locations with at least 10 days of matched pairs are shown.

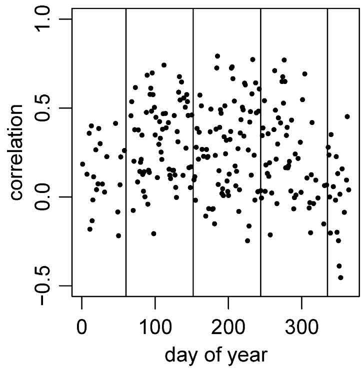

FIGURE 2. Correlations of AOD with $PM_{2.5}$ across space by day of year, requiring at least three retrievals per site-day and including only days with at least 30 such sites. Vertical lines divide the seasons.

There were no clear and substantial relationships between the correlations and local information about the site, such as land use, population density, monitoring objective, or local emissions. The results are robust with respect to various thresholds for the number of AOD retrievals required to calculate the daily average AOD and the number of days required to calculate the correlation at a site, although the correlations are lower when fewer retrievals are required in a day.

Because of the low correlations in the western U.S., we henceforth restrict our analyses to locations east of 100°W, which includes most of the counties violating the EPA air quality standard for $PM_{2.5}$ except for California.

Correlations over space (Figure 2) are less strong than those over time, suggesting that AOD can better distinguish high from low $PM_{2.5}$ over time at fixed locations than over space at fixed times. This may be related to spatially varying factors such as average reflectivity, aerosol type, or local meteorology that obscure, and potentially confound, the relationship between AOD and $PM_{2.5}$. The results are again robust with respect to various thresholds. Our calibration work (Section 3.3) suggests that the relationship between AOD and $PM_{2.5}$ varies by location, which helps to explain the low cross-sectional correlations seen here; after calibration based on location, the associations improve. The correlations again tend to be lower in winter; this cannot be explained by the minimal differences in the variability of $PM_{2.5}$ or AOD between winter and other seasons. Another possibility is that changes in reflectance with vegetation loss in winter may not be accurately captured by the retrieval algorithm.

3.3. Calibration Model Results. Here we focus on key results with respect to the importance of calibration and the relationships between AOD (either raw or calibrated) and $PM_{2.5}$ at different temporal resolutions. We calculated correlations at the daily scale as well as after averaging across available matched pairs within a month and within a year at each site-pixel match. Correlations are calculated only based on days for which both the AOD proxy and $PM_{2.5}$ were available, so we overstate the predictive ability of AOD for true monthly and yearly average $PM_{2.5}$, since there will be many days with no AOD retrievals. Our correlation results measure the ability of the AOD proxies to mirror heterogeneity in $PM_{2.5}$ over space and time.

On the daily scale model-calibrated AOD (equation 2) is more strongly correlated with $PM_{2.5}$ than the raw daily log average, $\log \bar{a}_{it}$ (Table 1). More importantly, without calibration, we cannot average over time and achieve more robust relationships; we discuss this surprising result below. Requiring a minimum number of AOD retrievals in a day improves associations over the shorter time periods. However, over the yearly period, by reducing the number of days with matched pairs, the resulting year-long averages are less robust and correlations decrease compared to using all days with at least one retrieval. Therefore, we suggest that analyses that average to monthly or yearly resolution include all available AOD retrievals. Comparisons using the held-out tenth set indicate that the model selection process described in the Supporting Information resulted in little overfitting.

TABLE 1. Correlations between both Raw and Calibrated AOD and $PM_{2.5}$ at Different Temporal Resolutions, Excluding Winter[a]

temporal resolution of correlations	(a) raw AOD ($\log \bar{a}_{it}$)	(b) calibrated AOD (a^*_{it})
Any Number of AOD Retrievals in a Day		
daily	0.41	0.50
monthly averages (at least 3 matched days for each site-month)	0.34	0.62
yearly averages (at least 10 matched days for each site)	0.17	0.75
At Least Five AOD Retrievals Each Day		
daily	0.51	0.59
monthly averages (at least 3 matched days for each site-month)	0.41	0.67
yearly averages (at least 10 matched days for each site)	0.19	0.69

[a] The two AOD proxies are (a) raw AOD, calculated using the log average daily AOD; (b) calibrated AOD (equation 2). Correlations are shown both when using matched pairs for days with any number of AOD retrievals and restricting to days with at least five retrievals.

The reduction in correlations between raw AOD and $PM_{2.5}$ when averaging over time mirrors the fact that correlations over time, holding space fixed, tend to be stronger than correlations over space, holding time fixed (Section 3.2). The within-site relationships between AOD and $PM_{2.5}$ are positive, but across sites and most noticeably at the yearly resolution, AOD is only weakly associated with $PM_{2.5}$. The most likely explanation is that there are spatially varying confounders that obscure the long-term average relationship between $PM_{2.5}$ and AOD, driving long-term average AOD down where long-term $PM_{2.5}$ is high and vice versa. The source of this confounding is unclear, but its effect is marked. The calibration, which is primarily driven by the spatial term (see Supporting Information), is able to account for the confounding. However, we caution that the correlation of calibrated AOD and $PM_{2.5}$ at the yearly level appears to be primarily driven by large-scale spatial patterns in both variables. The implication is that calibrated AOD may not help to improve long-term predictions when added to a $PM_{2.5}$ prediction model that relies on large-scale spatial smoothing of the monitoring data plus information from GIS and meteorological covariates.

In the Supporting Information, we compare the results with results from alternative calibration models, demonstrating that our chosen model (equation 1) has good relative performance.

Smooth Regression Functions. Figure 3 shows the fitted smooth regression functions of time, RH, PBL, and space for each of the three seasons. We interpret these functional relationships conditional on $PM_{2.5}$ being in the model. As expected, for a given concentration of $PM_{2.5}$, AOD increases with increasing PBL, since a higher PBL means the AOD retrieval is integrating over a longer column of air with reasonably homogeneous $PM_{2.5}$ concentrations. AOD increases with increasing RH (when RH is greater than 60−70%). The particle growth effect of humidity increases light extinction capability, thereby increasing AOD relative to ground-level $PM_{2.5}$, as the latter is measured as dry mass. The nonlinearity may occur because the growth effect of hygroscopic particles becomes more substantial with increasing RH (*19*). The wiggliness in the regression functions

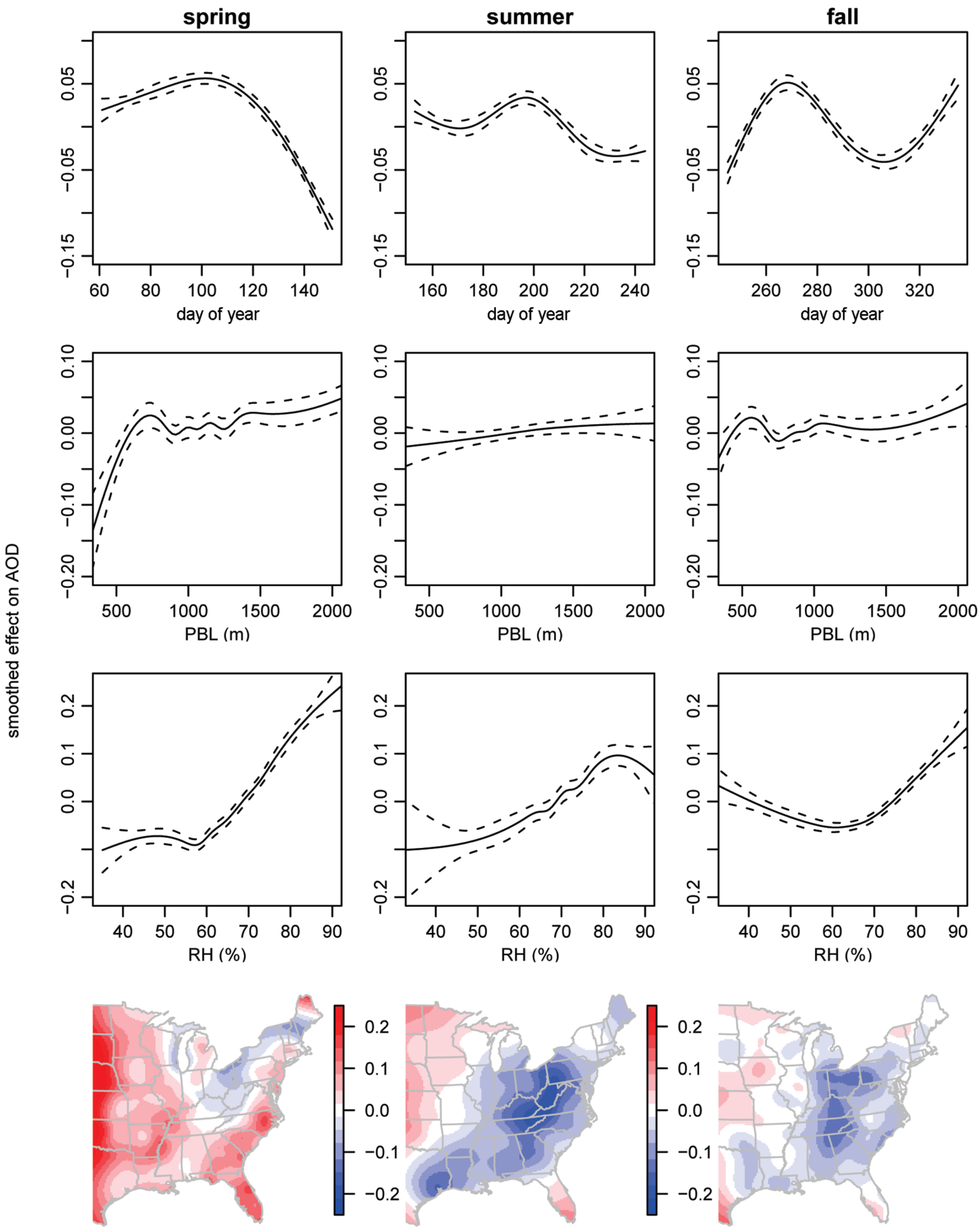

FIGURE 3. Fitted smooth regression relationships for the effects on AOD of (top row) time, $\hat{f}_t(t)$, (second row) PBL, $\hat{f}_{PBL}(PBL)$, (third row), RH, $\hat{f}_{RH}(RH)$, and (bottom row) space, $\hat{g}(s)$, by season. Larger values indicate that AOD is high relative to $PM_{2.5}$ for that value of the regression variable. In the spatial plots, red indicates that AOD is high relative to $PM_{2.5}$ and blue the converse. In the first three rows, dashed lines indicate pointwise 95% confidence intervals.

for PBL and RH likely reflects a moderate amount of overfitting from not fully accounting for within-site correlation in equation 1. The spatial patterns indicate that, holding $PM_{2.5}$ constant, we see low values of AOD over the Ohio River valley and Appalachian Mountains region. The lower than expected values of AOD may occur because large local emissions from power plants in the region increase the ratio of ground-level $PM_{2.5}$ to AOD. Spatial patterns may also be caused by additional meteorological factors, variability in aerosol type, and differences in the satellite viewing angle. Note that because RH and PBL vary in both space and time, this helps avoid concurvity and allows us to separate the effects of RH and PBL from effects of space and time.

3.4. Association between $PM_{2.5}$ and AOD Availability. Missingness of AOD retrieval may be associated with meteorological conditions that are also associated with pollution levels. If days with few or no AOD retrievals have systematically lower or higher average $PM_{2.5}$ than days with many retrievals, then missingness of AOD is itself informative about $PM_{2.5}$ and using only available AOD retrievals may bias predictions of $PM_{2.5}$. We investigate this based on the distribution of $PM_{2.5}$ as a function of the proportion of missing AOD retrievals.

Figure 4 (top row) shows the mean $PM_{2.5}$ by season as a function of the number of AOD retrievals. In summer, there is a marked difference in $PM_{2.5}$ concentrations as a function of AOD retrievals, with the highest concentrations on days with approximately 5−10 retrievals and lower concentrations for days with few retrievals. Spring shows a somewhat similar, but less marked pattern, while fall shows little systematic pattern.

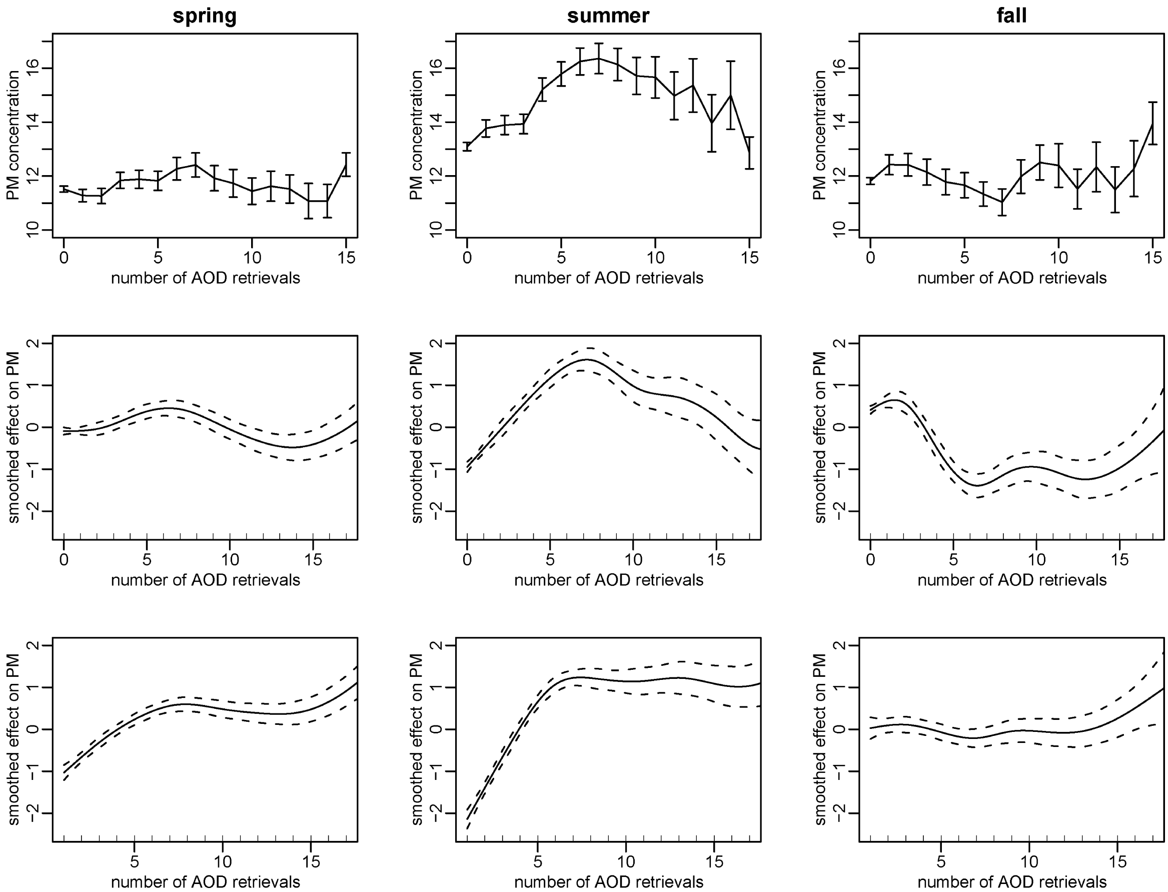

FIGURE 4. (Top row) Average $PM_{2.5}$ concentration (with 95% confidence interval) as a function of number of AOD retrievals by season. Data at the *x*-axis value of 15 are for 15 or more retrievals. (Middle row) Smoothed regression relationship between number of AOD retrievals and $PM_{2.5}$ by season, controlling for location, time, and meteorology (equation 4). (Bottom row) Smoothed regression relationship between number of AOD retrievals and $PM_{2.5}$ by season when at least one retrieval is made in day, controlling for location, time, meteorology, and average AOD in a model of the form in equation 4 but with a smooth term of average daily AOD also included.

Since $PM_{2.5}$ varies in space and time, as does missingness, the association between missingness and $PM_{2.5}$ may occur merely because both missingness and $PM_{2.5}$ are separately associated with location and time. We attempt to control for space, time, and meteorology by fitting the following generalized additive model separately for the spring, summer, and fall seasons.

$$\log \mathrm{PM}_{it} \sim N(\mu + g(s_i) + f_t(t) + f_{\mathrm{PBL}}(\mathrm{PBL}_{\mathrm{it}}) + f_{\mathrm{RH}}(\mathrm{RH}_{\mathrm{it}}) + f_n(n_{\mathrm{AOD},it}), \tau^2) \quad (4)$$

where $n_{\mathrm{AOD,i,t}}$ is the number of AOD retrievals for location i and day t. In Figure 4 (middle row) we see the fitted smooth regression function, $\hat{f}_n(n_{\mathrm{AOD}})$, for each of the three seasons, indicating a nonlinear relationship between number of retrievals and $PM_{2.5}$, with $PM_{2.5}$ increasing with increasing number of retrievals, reaching a peak, and then declining as the number of retrievals increases. This suggests that after controlling for other factors affecting $PM_{2.5}$, there is still a relationship between missingness and $PM_{2.5}$.

For those days with at least one retrieval, we can also control for measured AOD. Adding a smooth function of average AOD, $f_a(\bar{a}_{\mathrm{it}})$ to the model (equation 4) did not remove the association between missingness and $PM_{2.5}$ (Figure 4, bottom row), although it did change the relationships somewhat, with spring and particularly summer showing increases in $PM_{2.5}$ with increasing number of retrievals and then leveling off with a larger number of retrievals. Fall shows little relationship of $PM_{2.5}$ to number of retrievals after accounting for the observed AOD.

These results suggest that predictive modeling of $PM_{2.5}$ based on AOD should take the number of retrievals on a day into account as providing additional information about $PM_{2.5}$ concentrations. In particular, not accounting for missingness during the summer is likely to upwardly bias one's estimates of $PM_{2.5}$ because days with few or no AOD retrievals on average have low $PM_{2.5}$ concentrations.

4. Discussion

We report the first comparison of GASP AOD with ground-level $PM_{2.5}$, building upon the expanding literature comparing MODIS and MISR AOD with $PM_{2.5}$. We build calibration models that result in moderately strong correlations of calibrated AOD with $PM_{2.5}$ in the eastern U.S. except during winter. Correlations increase with averaging over longer time periods when using the calibrated AOD. We also point out that whether AOD retrievals are missing does not occur at random with respect to $PM_{2.5}$ concentrations, as has also been reported for MODIS (*20*).

The higher nominal spatial resolution of GASP AOD compared to MODIS and MISR does not appear to provide real improvement in spatial resolution, presumably because of instrument differences. Correlations of GASP AOD with $PM_{2.5}$ on daily basis found here are lower than found in studies (*10, 11*) when averaging over multiple MODIS and MISR pixels. However, given the limitations of the GOES instrument, the fact that the GASP AOD correlations are not too much lower than for MISR and MODIS indicates the promise of GASP AOD for use as a proxy for $PM_{2.5}$.

Critically, comparisons on a daily basis for matched $PM_{2.5}$ and AOD data do not take into account the much greater data density of GASP AOD. The half-hourly temporal coverage provides much more opportunity for avoiding clouds at least once during a day and for more robust estimates of daily pollution by averaging over noisiness in the retrievals and over temporal variability in pollution during the day. To estimate monthly average $PM_{2.5}$, the greater data density should result in proxy values that are more representative of $PM_{2.5}$ over all the days in the month than from MODIS and MISR, which we are assessing quantitatively in ongoing work. Finally, in the Supporting Information, we provide evidence that some of the criteria used to select valid GASP AOD retrievals might be relaxed to provide even more retrievals.

Of perhaps equal importance to its dense temporal coverage, GASP AOD provides the possibility of a long-term record starting in November 1994, when the GOES-8 satellite retrievals are first available. Dense $PM_{2.5}$ ground monitoring only began in 1999, so GASP AOD provides one of the few proxies for $PM_{2.5}$ for the period 1995−1998. For epidemiological work, improvements in exposure estimation for four years could increase statistical power to detect health effects.

This work is part of a larger project in which we will use GASP, MODIS, and MISR AOD integrated with ground-level $PM_{2.5}$ monitoring in a statistical model to estimate $PM_{2.5}$ at high spatial resolution across the eastern U.S. Further conclusions as to the relative usefulness of the different AOD products as proxies for $PM_{2.5}$ will be informed by the statistical modeling. This will involve a base model built using $PM_{2.5}$ monitoring data and GIS and meteorological covariates and expanded models that also include AOD retrievals. We believe the ultimate test is whether the addition of AOD retrievals improves upon predictions that could be made without the remote sensing information.

Acknowledgments

This work was supported by grant 4746-RFA05-2/06-7 from the Health Effects Institute. The authors thank Doug Dockery for helping to initiate the collaboration between NOAA and Harvard, Steve Melly for GIS processing, and Jeff Yanosky for suggestions. NARR data were provided by the NOAA/OAR/ESRL PSD, Boulder, CO, from their website at http://www.cdc.noaa.gov.

Supporting Information Available

Additional information on data availability and raw correlations, alternative statistical models, and sensitivity analysis of the criteria for valid GASP AOD retrievals. This information is available free of charge via the Internet at http://pubs.acs.org.

Literature Cited

(1) Dockery, D.; Pope, C.; Xu, X.; Spengler, J.; Ware, J.; Fay, M.; Ferris, B.; Speizer, F. An association between air pollution and mortality in six U.S. cities. *N. Engl. J. Med.* **1993**, *329*, 1753–1759.

(2) Pope, C.; Burnett, R.; Thun, M.; Calle, E.; Krewski, D.; Ito, K.; Thurston, G. Lung cancer, cardiopulmonary mortality and long-term exposure to fine particulate air pollution. *J. Am. Med. Assoc.* **2002**, *287*, 1132–1141.

(3) Pope, C.; Burnett, R.; Thurston, G.; Thun, M.; Calle, E.; Krewski, D.; Godleski, J. Cardiovascular mortality and long- term exposure to particulate air pollution: epidemiological evidence of general pathophysiological pathways of disease. *Circulation* **2004**, *109*, 71–77.

(4) Miller, K.; Siscovick, D.; Sheppard, L.; Shepherd, K.; Sullivan, J.; Anderson, G.; Kaufman, J. Long-term exposure to air pollution and incidence of cardiovascular events in women. *N. Engl. J. Med.* **2007**, *356*, 447–459.

(5) Yanosky, J.; Paciorek, C.; Schwartz, J.; Laden, F.; Puett, R.; Suh, H. Spatio-temporal modeling of chronic PM10 exposure for the Nurses' Health Study. *Atmos. Environ.* **2008**, *42*, 4047–4062.

(6) Samet, J.; Dominici, F.; Curriero, F.; Coursac, I.; Zeger, S. Particulate air pollution and mortality: findings from 20 U.S. cities. *N. Engl. J. Med.* **2000**, *343*, 1742–1757.

(7) Dominici, F.; Peng, R.; Bell, M.; Pham, L.; McDermott, A.; Zeger, S.; Samet, J. Fine particles, air pollution and hospital admission for cardiovascular and respiratory diseases. *J. Am. Med. Assoc.* **2006**, *295*, 1127–1135.

(8) Wang, J.; Christopher, S. A. Intercomparison between satellite-derived aerosol optical thickness and PM2.5 mass: Implications for air quality studies. *Geophys. Res. Lett.* **2003**, *30*, 2095.

(9) Engel-Cox, J.; Holloman, C.; Coutant, B.; Hoff, R. Qualitative and quantitative evaluation of MODIS satellite sensor data for regional and urban scale air quality. *Atmos. Environ.* **2004**, *38*, 2495–2509.

(10) Liu, Y.; Sarnat, J.; Kilaru, V.; Jacob, D.; Koutrakis, P. Estimating ground-level PM2.5 in the eastern United States using satellite remote sensing. *Environ. Sci. Technol.* **2005**, *39*, 3269–3278.

(11) Liu, Y.; Franklin, M.; Kahn, R.; Koutrakis, P. Using aerosol optical thickness to predict ground-level PM2.5 concentrations in the St. Louis area: a comparison between MISR and MODIS. *Remote Sens. Environ.* **2007**, *107*, 33–44.

(12) Pelletier, B.; Santer, R.; Vidot, J. Retrieving of particulate matter from optical measurements: a semiparametric approach. *J. Geophys. Res.* **2007**, *112*, D06208.

(13) Kahn, R.; Banerjee, P.; McDonald, D.; Diner, D. Sensitivity of multiangle imaging to aerosol optical depth and to pure-particle size distribution and composition over ocean. *J. Geophys. Res.* **1998**, *103*, 32195–32213.

(14) Prados, A.; Kondragunta, S.; Ciren, P.; Knapp, K. GOES aerosol/smoke product (GASP) over North America: comparisons to AERONET and MODIS observations. *J. Geophys. Res. Atmos.* **2007**, *112*, D15201.

(15) Knapp, K.; Haar, T. V.; Kaufman, Y. Aerosol optical depth retrieval from GOES-8: Uncertainty study and retrieval validation over South America. *J. Geophys. Res.* **2002**, *107*, D4055.

(16) Rogers, R.; Kondragunta, S.; McQueen, J.; Moshary, F.; Gross, B.; Hoff, R. Validation of CMAQ-modeled planetary boundary layer height with elastic lidar; 7th ISTP Symposium, Boulder, CO, June 2006.

(17) Wood, S. *Generalized Additive Models: An Introduction with R*; Chapman & Hall: Boca Raton, 2006; p 391.

(18) Chin, M.; Diehl, T.; Ginoux, P.; Malm, W. Intercontinental transport of pollution and dust aerosols: implications for regional air quality. *Atmos. Chem. Phys.* **2007**, *7*, 5501–5517.

(19) Chin, M.; Ginoux, P.; Kinne, S.; Torres, O.; Holben, B.; Duncan, B.; Martin, R.; Logan, J.; Higurashi, A.; Nakajima, T. Tropospheric aerosol optical thickness from the GOCART model and comparisons with satellite and sun photometer measurements. *J. Atmos. Sci.* **2002**, *59*, 461–483.

(20) Koelemeijer, R.; Homan, C.; Matthijsen, J. Comparison of spatial and temporal variations of aerosol optical thickness and particulate matter over Europe. *Atmos. Environ.* **2006**, *40*, 5304–5315.

ES703181J